Available Online at http://www.journalajst.com

ASIAN JOURNAL OF SCIENCE AND TECHNOLOGY

ISSN: 0976-3376

Asian Journal of Science and Technology
Vol. 6, Issue 04, pp. 1311-1315, April, 2015

RESEARCH ARTICLE

MODIFICATION ON THE SYNTHESIS PROCESS OF HYDROXYAPATITE

***Dora E. Ledesma-Carrión**

Instituto Politécnico Nacional UPALM- Zacatenco, C.P. 07738, México, D.F. MÉXICO

ARTICLE INFO

Article History:
Received 27th January, 2015
Received in revised form
28th February, 2015
Accepted 15th March, 2015
Published online 30th April, 2015

Key words:
Synthetic Hydroxyapatite,
Stoichiometric com- pound,
Nanometer range,
Pore size,
Particle size.

ABSTRACT

A rod-like morphology with particle size of 20-50x100-200 nm, particle average size of 175.9 nm with 1-modal, pore radii of 1.22 nm and stoichiometric and anisotropic hy- droxyapatite (HA) was prepared by reacting calcium hydroxide and a phosphoric acid solution. The resulting powder was heat treated at 680° C. Two time of aging were applied at 24 and 48 h. This process does not include sintering only heat treatment, and it is a HA fabrication advantage. And this does not present oxides or some carbonates traces. This method is easier and cheaper than reported originally [1] due to synthesis process which does not involve controlled atmosphere in the reactor at room temperature. The particles characteristics are single and homogeneous in phase, uniform particle size in the nanometer range and chemical composition [2], [8]. The prepared hydroxyapatite has similar properties in comparison with the originally reported in relation to morphology, particle size and stoichiometric compound.

INTRODUCTION

Hydroxyapatite (H A, $Ca_5(PO_4)_3(OH)$) has hexagonal-bipyramidal symmetry and its properties depend on the synthesis method. The synthetic HA is produced by the precipitation of precursors (Afshar *et al* 2003, Yeong *et al.,* 1999, García *et al.,* 2006 and Guzmán *et al.,* 2005). There are many impact factors over HA properties and qualities. The main factors are: drip frequency, stir speed, times of aging and drying and temperature rate (Afshar *et al*., 2003 and Juang *et al.,* 1995). Pore and particle size of produced HA are important because they affect the quality. In the case of natural bone made HA, the crystal size is of 1-7 µm and the pore size is 0.1-500µm (Joschek *et al.,* 2000). The dimensions of crystals in native bone have been reported to be on the order of 20-40 x 20-40 x 2.5-5 nm (Joschek *et al.,* 2000). This synthetic HA pore and particle size is 3 magnitude orders less than the bovine bone manufactured HA. Therefore, heat treatment has to be applied to HA powder before cold isostatic pressure (CIP) or uniaxial compacting or sintering. Other method at room temperature was prepared using the precipitation of the same precursors (method of Rathje (Juang *et al.,* 1995)) and com- pacting in a uniaxial die (diameter:1 cm, pressure 25 MPa), followed by heat treatment, before using a cold isostatic pressure (CIP) and sintering at high temperature of 1000° C for $>$ 7h.

Corresponding author: Dora E. Ledesma-Carrión
Instituto Politécnico Nacional UPALM- Zacatenco, C.P. 07738, México, D.F. MÉXICO.

In this case, pH was controlled using concentrated ammonia solution, time of aging for $>$ 48 h, drying at 50° C for 72 h, washed using deionized water several times. Heat treatment rate was of 5° C/min up to 350° C for 2h (Yeong *et al.,* 2001). Particles morphology is dendrite-shaped agglomerates. Others (García *et al.,* 2006) propose to begin with calcium nitrate aqueous solutions ($Ca(NO_3).4H_2O$) and ammonium phosphate ($H_2(PO_4)NH_4$), times of aging (115 h) and resting (5 days), sintering temperature (1 h, 1050° C), and heat treatment (15 h). The precipitated HA presents phosphates and nitrates compounds and amorphous phase. In this case, it is necessary ideal conditions for getting pure HA (García *et al.*, 2006).

Experiment Details

The modifications made to the original synthesis reported (Afshar *et al.,* 2003) were: the synthesis process was made at room temperature and consisted on the addition of a phosphoric acid (H_3PO_4) solution diluted in deionized water to a calcium hydroxide ($Ca(OH)_2$) solution diluted in distilled water. The controlled factors were pH until getting $9-10$, stirring speed $6-7$c/s, drop wise frequency 2 $\text{drops/s} = 0.1\text{ml/s}$ at $20\text{ml}/30\text{min}$, ageing time 48 h, the dried time 48 h at 110° C and the powder was heated for 3 h at 680° C using argon atmosphere from 500° C to 680° C with nitial and terminal temperature rate of 10° C/min. The other main modifications made on the synthesis process were:

- without addition of ammonium hydroxide (NH_4OH).
- The precipitated was decanted 12 h after, washed with
- deionized water and filtered by gravity with paper filter twice.
- There is not post-chemical treatment.
- There is not uniaxial compaction or CIP before heat treatment (Yeong *et al*., 1999, 2001 and Mostafa *et al*., 2005).

The average particle size was measured in a Zetasizer nano-Z5 analyzer. Samples consist on 0.01 g HA diluted in 20ml alcohol and subjected to ultrasonic vibration for 30min before measurements were made. The Raman normal vibration modes were measured with Spectrometers Nicol*et al* mega XR Dispersive Raman Thermo Electron Corporation (laser 532nm, 100% power) and IR modes were studied with Nicolet Nexus 670 FT-IR Thermo Electron Corporation OMNIC (KBr 99% HA 1%), HA pills were 1 cm of diameter and 0.1 g. A Furnaces Felisa ($0-220^{\circ}C$) and 6000 Thermolyne ($0-999^{\circ}C$), were respectively used for the powder drying and heat treatment. The morphology and chemical compound were observed in powder samples through SEM Stereoscan 440 (20 KV, 250 pA) and SEM-HR FEI Quanta 3D FEG (10 KV, 93.3 pA, x75000.

Also a TEM Jeol JEN 1200 EX (120 KV). XRD Bruker 8 Advance D8 (30 KV, 40 mA) were used. The TGA/DSC studies were carried out by a TA-Instruments, model STD Q600, using a standard aluminum pan at a heating rate of $10^{\circ}C\,min^{-1}$ on air from $20^{\circ}C$ up to $695^{\circ}C$ temperature range. Porosity was studied with a BET-BJH test. This study was performed in Minisorp II BEL-Japan with an activation temperature of $110^{\circ}C$ in vacuum. Isothermal at 77K for 24 h. For analysis and calculi Langmuir adsorption equation was used. Later statistic analysis was applied to data.

RESULTS AND DISCUSSION

To verify the purity of HA Figure 1 shows a HA with ageing time of 24 h, XRD pattern in single and homoge- neous phase (PDF 86-1199) with a refine microstructure, no-stoichiometric compound with a little XRD picks displacement in the 2θ range from 6° to 90°. On the other hand, with ageing time of 48 h, the XRD pattern (from 6 to 70° in 2θ) showed a stoichiometric compound with a single phase (PDF 89-4405). In both patterns do not appear CaO plane (200) pick, thus, there is not HA contamination or breakdown with (cc)/without (sc) heat treatment, this can be observed in Figure 2.

Table1Bjhanalysis of ha sc vs ha cc. Ha cc reduced it sporearea and volume over 50% and it spick oreradii, 35.1%.

Plot data HA sc	Adsorption branch	Plot data HA cc	Adsorption branch	Plot data HA sc vs cc	Adsorption branch
V_p	$0.1758[cm^3g^{-1}]$	V_p	$0.061055[cm^3g^{-1}]$	V_p	65.3%
$r_{p,peak}$(Area)	$1.88[nm]$	$r_{p,peak}$(Area)	$1.22[nm]$	$r_{p,peak}$(Area)	35.1%
a_p	$68.665[m^2g^{-1}]$	a_p	$32.53[m^2g^{-1}]$	a_p	52.6%

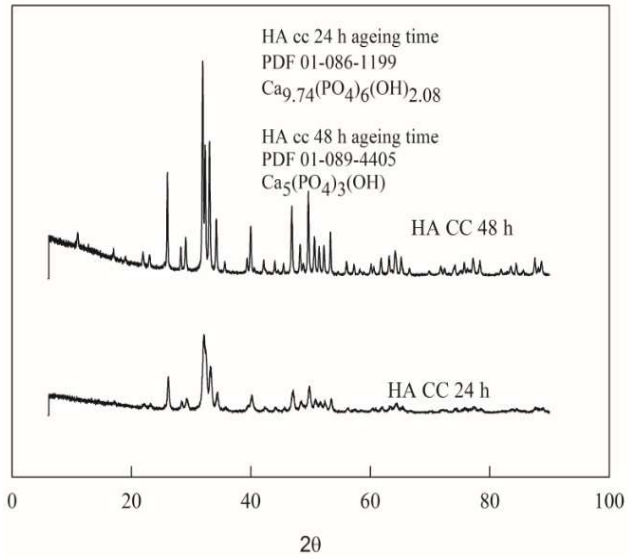

Fig 1. XRD of HA with time of aging of 24 h and 48 h with heat treatment.

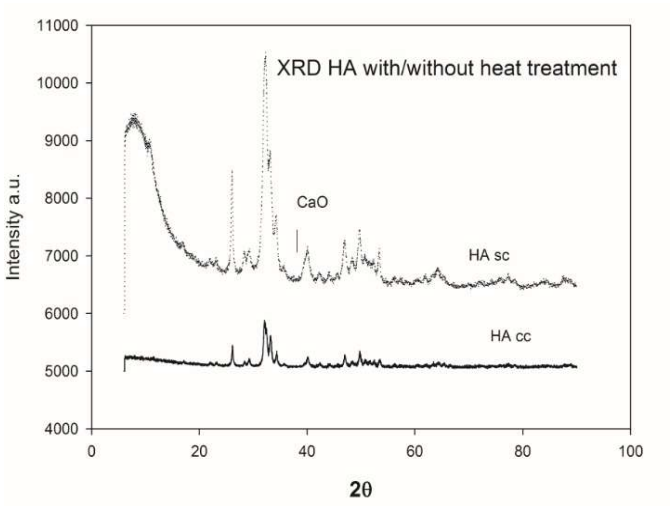

Fig 2. XRD of HA sc vs HA cc. HA sc shows amorphous phase. HA cc does not present oxides or carbonates. The XRD patterns of HA do not show CaO pick planes (200).

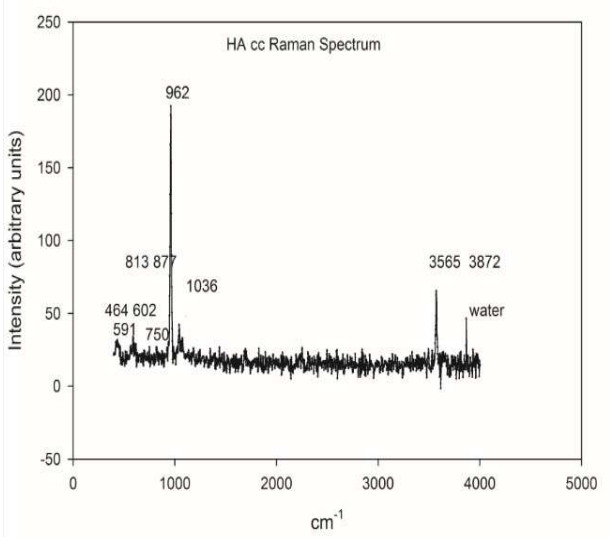

Fig. 3. Raman Spectrum of HA cc: Typical Raman spectrum of typical synthetic HA. The normal vibration modes are observed in the spectrum.

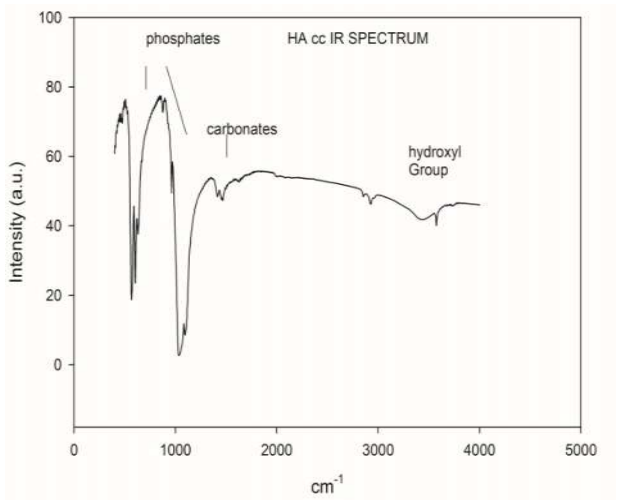

Fig 4. IR Spectrum of HA cc: Typical IR spectrum of typical synthetic HA. Hydroxyl group and Phosphate and carbonates bands are observed in the spectrum.

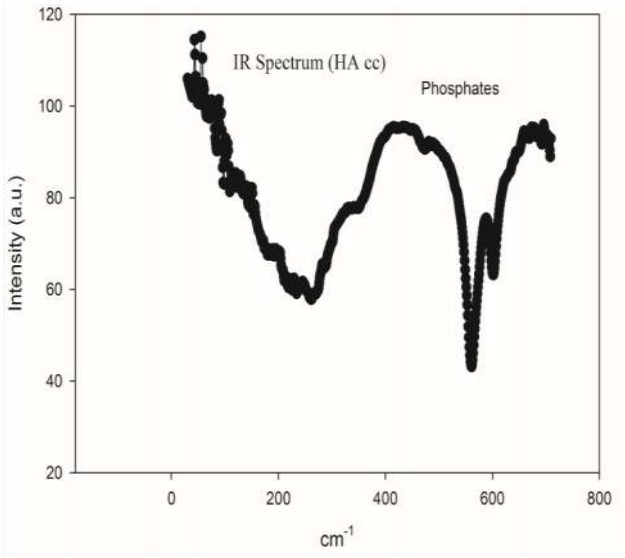

Fig. 5. IR near Spectrum of HA cc: Typical IR spectrum of typical synthetic HA. Phosphate bands are observed in the spectrum.

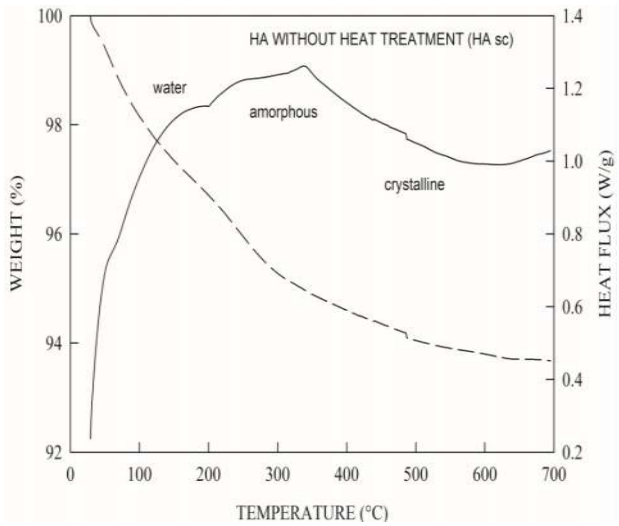

Fig 6. TGA-DSC of HA sc shows an amorphous phase before at 480° C.

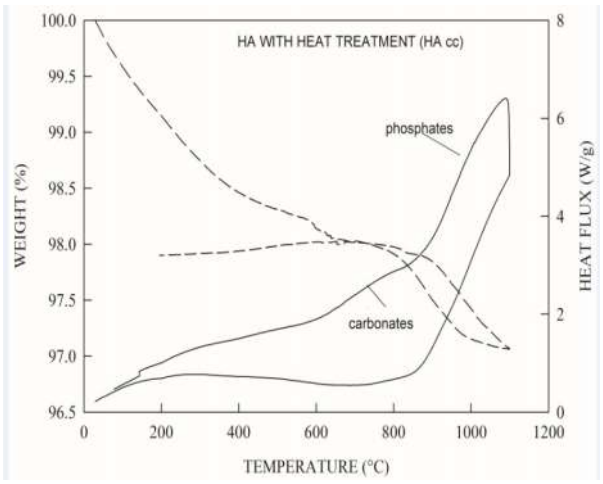

Fig 7. TGA-DSC of HA cc does not show an amorphous phase. HA cc presents a breakdown in carbonates and phosphates.

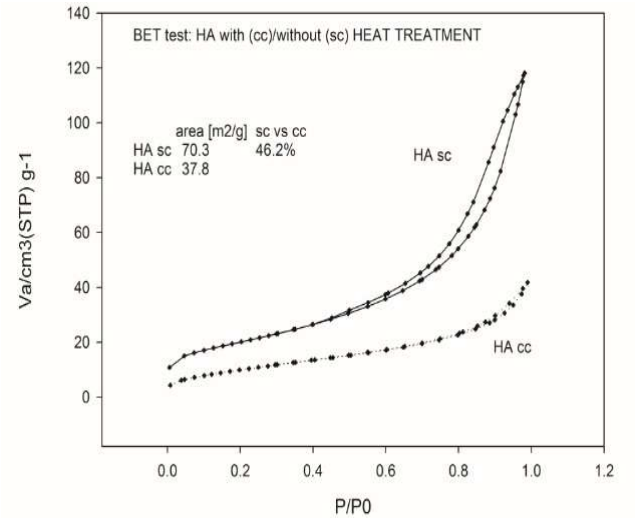

Fig 8. BET test: HA sc vs HA cc, both cases HA show mesoporosity. HA cc reduced its total area 46.2%.

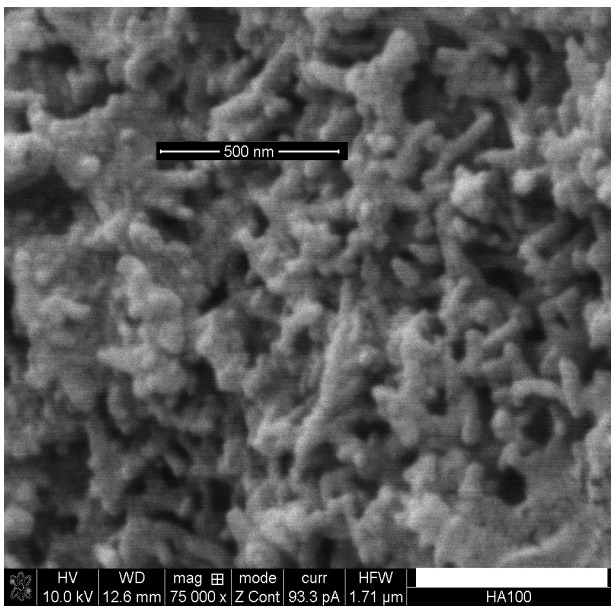

Fig 9. SEM-HR showed cylinder rods morphology (X75000) length □ 200nm and diameter □ 20nm.

Fig 10. TEM sets nano-crystalline (particles 20-100 nm) HA cc.

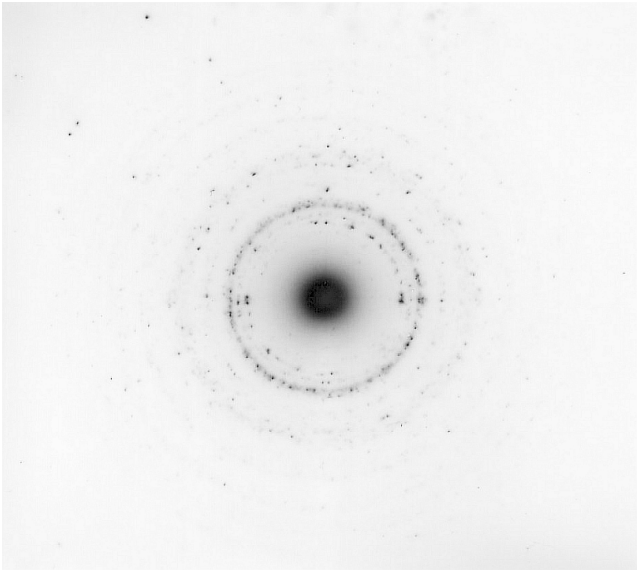

Fig 11. TEM electron diffraction set nano-crystalline HA cc and light texture.

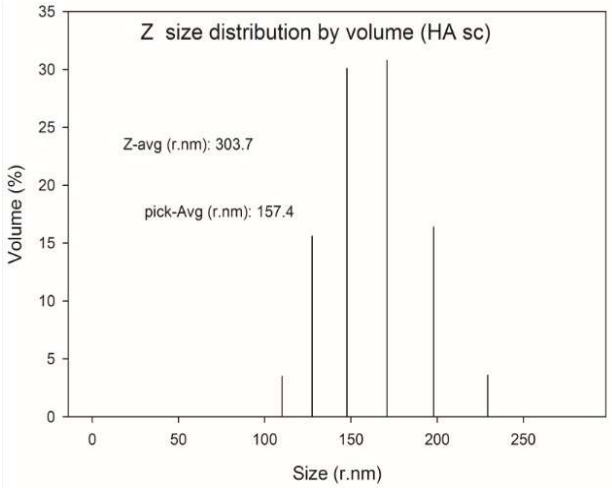

Fig 12. HA without heat treatment average size distribution 1-modal

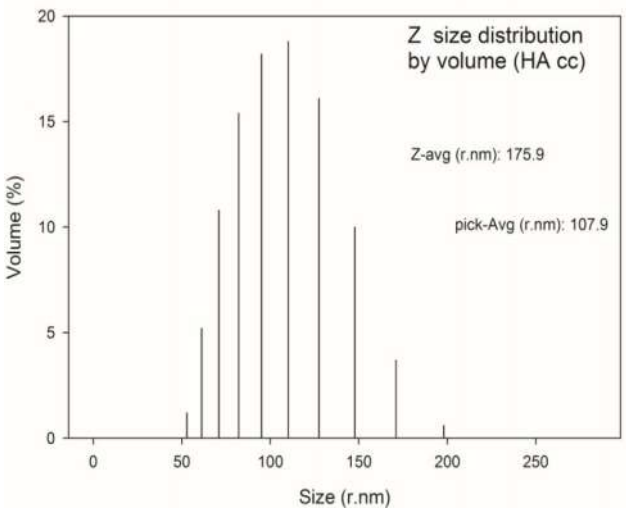

Fig. 13. HA with heat treatment Z-size average distribution 1-modal. HA cc reduced particle size average 42.08%.

HA is reported with CaO plane pick (Afshar *et al.,* 2003, Yeong *et al.,* 1999, 2001, Mostafa *et al.,* 2005 and Juang *et al.,* 1995) arguing that the FTIR results show an intense carbonate band (υ_3 carbonate bands $1450 - 1550 cm^{-1}$). The HA powder easily host a carbon dioxide substitution in its crystal structure. Carbonate ions $(CO_3)^{2-}$ can substitute hydroxyls or phosphates sites and based on this, carbonated HA type A and type B, respectively, formed (Afshar *et al.,* 2003). So, in order to reach a pure HA precipitate with traces of carbon dioxide contamination, it is effective to use controlled atmosphere during precipitation process. This is verified with Raman and Infrared spectra results, Figure 3, Figure 4 and Figure 5, showed characteristic absorption bands of HA cc (Rehman *et al.,* 1997), two strong band and four vibration modes regions. No-stoichometric HA ($Ca/P < 1.67$) is made with this method (Guzmán *et al.,* 2005). Phosphate bands: Theoretically, there are four normal vibration modes present for phosphate ions. All these modes are Raman and infrared active and are observed for all the spectra of hydroxyapatite powders. Hydroxyl bands: Hydroxyl stretch is observed at 3569 cm^{-1} and a hydroxyl band at 624 cm^{-1}. Phosphate ν_1 band is observed in the region of 475 and 440 cm^{-1} and has only one site in 472 cm^{-1}. Phosphate ν_2 band is at 961-2 cm^{-1} and can be observed in all the spectra of hydroxyapatite. The ν_3 band has three different sites at 1096, 1085 and 1056 cm^{-1}. Phosphate ν_4 band is in the region of 660 and 520 cm^{-1} and is a well-defined and sharp band. The hydroxyapatite spectra have observed three sites at 633, 602 and 566 cm^{-1}. IR spectrum shows a low intensity carbonate band ~ 1500 cm^{-1}. This indicates that carbonate HA or oxide traces appear in the IR plot. Then HA had not a breakdown. The results reveal that the carbonate content is directly related to Ca/P ratio (Afshar *et al.,* 2003). Original reported Ca/P is in the range of $1.659 - 1.970$ (Afshar *et al.,* 2003). Then the HA had a breakdown. In this study the C/P average $= 1.67 \pm 0.04$. These results are in agreement with SEM-EDS, XRD and T GA/DSC 4 results. The breakdown effect without a controlled atmosphere (Feng-Huei *et al.,* 2000)

is showed in figure 6 and figure 7. This is analyzed by TGA/DSC in air showing water lost and formation of amorphous HA sc ~ 350° C and crystalline ~ 480° C. HA cc had carbonates breakdown at ~ 700° C and phosphates at~ 850° C. So the heat treatment was made at 680° C in Ar atmosphere to avoid breakdown. To verify pore size in a nanometer range in figure 8 and table I appear Nitrogen-Adsorption-desorption (BET) tests. These showed mesoporosity (curves type II, (Sing *et al.,* 1985 and Condon *et al.,* 2000)) with a total surface area of 37.8m^2 /g, pore volume V_p of 0.061055cm^3 /g after heat treatment. The porosity was reduced to ~ 46% (total surface area: 70.3m^2 /g, V_p = 0.1758cm^3 /g before heat treatment). The BJH test results show $r_{p,\,peak}$ (peak pore radii) and a_p (pore area) reduced to 65.3% and 52.56%, respectively. The $r_{p,\,peak}$ reduced from 1.88 to 1.22 nm and a_p from 68.67 to 32.53 m^2 /g (Sing *et al.*, 1985 and Rouquérol *et al.,* 1994). The rod-like morphology and chemical compound were verified by scanning and transmission electron microscopes results and presented in figure 9 and figure 10.

These results showed a particle size ranging from 20 to 200 nm, and HA electron diffraction analysis presented a light textured in c-axe. SEM-HR micrograph (x75000) indicates that the precipitated particles have a rod-like morphology with ~ 200 nm in lateral and ~ 20nm in diameter dimensions. SEM- EDX analysis set Ca/P average ration 1.668. Maximum: 1.708, Minimum: 1.629. This range is smaller than reported HA (Afshar *et al* 2003). On the other hand, Z-size average distribution test have several results: particle size average de- creases 42.08% from 303.7 to 175.9 nm after heat treatment. These data are in concordance with TEM and SEM studies. Moreover, to verify HA anisotropic behavior in figure 11 light texture evidence is observed in TEM-electron diffraction pattern. This shows nano-crystalline diffraction rings structure and a ring spacing characteristic in the hexagonal structure sequence. The preferred orientation is on c-axis. Thus the HA growing structure follows this direction because of Ca-Ca bond is parallel to the c-axis (hardness effect and Ca-OH bond is perpendicular (damping effect, (Gó mez *et al.,* 2004 and, Neder *et al.,* 1996)). Homogeneity is observed in figure 12 and figure 13 based on the distributions 1-modal type. This result is different from the reported (Yeong *et al* 1999, 2001 and Mostafa *et al.,* 2005). Theses show distribution types 2-modals and 3- modals and particle average size of 0.9-45 μm (Mostafa *et al.,* 2005).

Conclusions

The synthesized HA is anisotropic in c-axis direction and stoichiometric (Ca/P = 1.67). It consists of 20-50x100-200 nm rod-like morphology. It shows carbonate traces only. There is thermal stability after heat treatment with Ar atmosphere. The main factor to get stoichiometric HA is time of aging (48 h). The heat rate (10° C/min) determines particle size and drip frequency (0.1ml/s) that fits pH level (9-10).

The heat treatment impacts on pore size (1.22nm) and particle size (175.9nm), and in particles morphology whenit is applied before compacting. If the order is reverse, the pressure generates dendrite shapes because of strain-stress forces. It is recommender heat treatment before compacting. This method is more economic than others (Afshar *et al*., 2003, Juang *et al.,* 1995, García *et al.,* 2006 and Guzmán *et al.,* 2005) because it reduces synthesized HA procedures times, controls factors and gets good quality.

Acknowledgements

The author would like to thank PhDs Prof. Heriberto Pfeifer, Omar Novelo-Peralta, Carlos Flores-Morales, Este- ban Fregoso, Mayahuel Ortega, Hugo Martínez, S.M. Jorge Osorio-Fuente, M.T.L. Muciño-Porras, Ana Dueñas-Pérez and Lidia Hernández-Hernández for your help and support in the characterization process.

REFERENCES

Afshar, A., Ghorbani, M., Ehsani, N., Saeri, M. R. and Sorrell, C. C. 2003. Materials and Design, Vol. 24, pp. 197-202,.

Condon, J.B. 2000. Microporous Mesopourus Mat., Vol. 38, pp. 359-383.

Feng-Huei, L., Liao Ch, J., Ko-Shao Ch. and Jui-Sheng S. 2000. Materials Science and Engineering C, Vol. 13, pp. 97-104.

Garcia, C., Paucar, C. and Gaviria, J. "Study of some parameters that determine the synthesis of hydroxyapatite by the precipitation route", Dyna rev.fac.nac.minas [online], vol.73, n.148, pp. 9-15, ISSN 0012-7353, 01/06.

Gómez Ortega JL, Villarreal Elizondo N, Guerrero Villa HM. Crystalography visualization of hydroxyapatite [Visualización cristalográfica de la hidroxiapatita]. Ingenierías. 2004;7(24):46-50.

Guzmán, C., Pia, C. and Munguía, N. 2005. Rev. Mex. Fis., Vol. 51, pp. 284-293.

Joschek, S., Nies, B., Krotz, R. and Gpferich, A. 2000. Biomaterials, Vol. 21, pp. 1645-1658.

Juang, H. Y. and Hon, M. 1995 H., Biomaterials, Vol. 17, pp. 2059-2064, 1995.

Mostafa N. Y., Materials Chemistry and Physics, Vol. 94, pp. 333-341, 2005.

Neder, N.B. and Proffen, Th., J. 1996. Appl. Cryst. Vol. 29, pp. 727-735. Würzburg Universität.

Rouquérol, J., Avnir, D., Fairbridge, C.W., Everett, D.H., Haynes, J.H., Pernicone, N., Ramsay, J.D.F., Sing, K.S.W. and Unger K.K. 1994. Micropore 2nm, mesopores 2-50 nm and macropores >50 nm in the BET and BJH Tests. Pure and Appl. Chem. IUPAC, Vol. 66, No. 8, pp. 1739-1758.

Rehman, I. and Bonfield, W. 1997. Journal of Materials Science: Materials in Medicine, Vol. 8, pp. 1-4, 1997.

Sing, K.S.W., Everett, D.H., Haul, R.A.W., Moscou, L., Pierotti, R.A., Rouqurol, J. and Siemieniewska, T., Pure and Appl. Chem. IUPAC, Vol.57, No. 4, pp. 603-619, 1985.

Yeong, K.C.B., Wang, J. and Ng, S.C. 1999. Materials Letters, Vol. 38, pp. 208-213.

Yeong, K.C.B., Wang, J. and Ng, S.C. 2001. Biomaterials, Vol. 22, pp. 2705-2712.

****